DEVELOPMENT OF DATA ACQUISITION DEVICES FOR ELECTRICAL IMPEDANCE TOMOGRAPHY OF COMPOSITE MATERIALS

Gschoßmann S.[1], Zhao Y.[2], Schagerl M.[3]

[1]Institute of Constructional Lightweight Design, Johannes Kepler University, Linz, Austria
Email: sandra.gschossmann@jku.at, Web Page: http://www.ikl.jku.at
[2]CD-Laboratory for Structural Strength Control of Lightweight Constructions, Linz, Austria
Email: yingjun.zhao@jku.at, Web Page: http://www.ikl.jku.at/laboratory
[3]Institute of Constructional Lightweight Design, Johannes Kepler University, Linz, Austria
Email: martin.schagerl@jku.at, Web Page: http://www.ikl.jku.at

Keywords: structural health monitoring (SHM), electrical impedance tomography (EIT), data acquisition system, carbon nanotube

Abstract
This contribution presents a simple and low-cost possibility to build a stand-alone data acquisition device to collect boundary voltage responses for electrical impedance tomography (EIT) evaluation. EIT reconstructs the spatial conductivity distribution of a region using boundary voltage responses to a current passing through the space. To accommodate EIT's application as a structural health monitoring technique, a hardware device for injecting current and acquiring data is developed. The hardware consists of three main devices: a current source that can generate a direct current in range of mA, a multi-channel voltmeter with desired precision, and a microcontroller that communicates between the device and the computer. In this study a Howland current source and a 16-channel CMOS-switch, both are controlled by an Arduino™ microcontroller, are developed to regulate the current and voltage connections. A MATLAB® GUI is developed to adjust current input, monitor the voltage measurement, and perform EIT reconstruction with embedded EIT algorithm EIDORS. With the aid of the GUI, one can perform quasi real-time EIT evaluation of a 16-electrode spatial area within 9 s. A paper folding test is performed to validate the functionality of the system, indicating that the performance of the device is adequate for structural health monitoring purposes.

Excerpt from ISBN 978-3-00-053387-7

1. Introduction

In order to ensure the safety of a composite lightweight structure within its service life, the application of structural health monitoring (SHM) systems can be a promising approach to receive early signs of material deterioration. Several fatal accidents in the past caused by structural failure of airplanes, trains or civil structures could have possibly been prevented if a reliable health monitoring system were in service. For example the Aloha Airlines Flight 243 incident in 1988 was caused by unattended accumulation of fatigue damages around panel joints that eventually led to the disassociation of the aircraft's upper fuselage shell during flight [1]. The Eschede train derailment in 1998, too, was caused by negligence of early fatigue wear in the train wheels [2]. These incidents have inspired numerous research on developing non-destructive testing methods and on-board SHM systems for ensuring the safety and reliability of public transportation and infrastructures.

During early ages of SHM development the sensor technology was not as advanced as today. Therefore strain gauges and other local strain monitoring devices were mostly used and a large amount of sensors had to be applied to monitor a large structure during its service life. Recent advancements in sensor technology offers opportunities to measure strain states along a curve through a fiber optical sensor; comparing to a strain gauge network, only a few sensors are needed to monitor a given area for the same sensing resolution. Current research on SHM sensor development are interested in direct measurement of the global behavior of a structure for evaluating its condition. For example Giurgiutiu [3] uses Lamb waves to identify the existence, location and severity of a damage over the wave-propagated region. These guided elastic waves, generated by piezoelectric transducers, can travel over long distances in thin-walled structures, whose interior condition influences the mode shape of the wave. Therefore with appropriate sensor arrangement, such a sensor network is able to detect and locate a damage in a thin-walled structure. Another technique to observe the global status of a given area is the electrical impedance tomography (EIT) [4]. This method reconstructs the spatial conductivity of a defined space using its boundary voltage responses to a current excitation. While coupled with a piezoresistive thin film sensor, the reconstructed map can visualize the location and severity of any strain-invoked damages within the given region. To perform an EIT evaluation, several electronic devices are needed to automate the data acquisition procedure, including a current source, a voltage measurement device and a multi-port switch that can be controlled via a centralized controller. This paper presents a simple and low-cost way to build a stand-alone data acquisition system that 1) injects current excitation, 2) reads and writes boundary voltage responses to computers, and 3) performs quasi real-time EIT reconstruction. An inkjet-printed carbon nanotube thin film is used as the strain-sensitive spatial damage sensor, and an open-source EIT algorithm EIDORS is adopted for reconstruction calculation.

2. Electrical Impedance Tomography

Practical EIT analysis was first found in biomedical applications. The first EIT measurement device, the Sheffield Mark I, was developed by Barber and Brown in early 1980s. It has been used to monitor and assess regional lung function [5]. Studies indicate that the spatial impedance changes if the thoracic air content changes; therefore irregularities in regional lung aeration and ventilation can be interpreted from the conductivity mapping. Due to its global monitoring perspective, EIT is also foreseen to have great potentials in structural health monitoring. Given a body Ω with a conductivity distribution σ, the current density J over the body can be expressed as

$$J = -\sigma \nabla \phi \tag{1}$$

where $-\nabla\phi$ is the electrical field over Ω. According to the Laplace's equation, the summation of J within Ω shall be equal to zero, or

$$\nabla \cdot \sigma \nabla \phi = 0 \tag{2}$$

Therefore if a defined current is injected to pass through the body, a unique voltage response, V, can be measured at discrete points along the boundary, such that

$$V_\mathrm{i} = \phi + z_\mathrm{i}\, \sigma \frac{\partial \phi}{\partial n} \tag{3}$$

where V_i is the voltage drop on the ith electrode, whose contact impedance is z_i, and n is the unit vector normal to the boundary. However, to recover the spatial conductivity distribution σ from V becomes an inverse problem, which is usually ill-posed and thus challenging to solve via direct inversion. Typical solvers for inverse calculation perform a least-squares fitting to find an estimated solution, σ^*, which satisfies the following functional

$$\min \left(\|V - V^*\|^2 + \alpha \, \|L(\sigma^*)\|^2 \right) \tag{4}$$

Excerpt from ISBN 978-3-00-053387-7

where $\alpha \|L(\sigma^*)\|^2$ is a generalized regularization term helping to smooth the calculation. A finite-element-based iterative approach can solve for an estimated solution σ^*, but it requires vast computational power and is therefore time-consuming. Instead of solving for the absolute conductivity, a relative contrast change of the conductivity based on its original state, $\frac{\Delta\sigma}{\sigma_o}$, can be reconstructed rapidly through a one-step inversion,

$$\frac{\Delta\sigma}{\sigma_o} = (H^T W H + \lambda R)^{-1} (H^T W) \frac{\Delta V}{V_o} \tag{5}$$

where $\frac{\Delta V}{V_o}$ is the contrast of boundary voltage response, H is the Jacobian matrix between V and σ from the forward calculation (*i.e.*, it is the forward calculation based on a presumed input value of σ, and the result becomes the initial input for the iterative approximation to start), W is the weighing matrix, R is the regularization term, and λ is the hyperparameter to control the magnitude of R. According to Adler *et al.* [6], the hyperparameter is determined by equating the signal-to-noise ratio of the input signal to that of the output signal.

It is obvious that the number of boundary voltage measurements determines the resolution of the reconstruction; therefore measurements are preferably taken under a complex current injection pattern. In this study a 16-electrode spatial configuration is chosen to perform EIT evaluation, as seen in Fig. 1. The boundary voltages are taken under 16 current injection scheme, resulting in a total of 256 data points for every reconstruction. More details on the current injection pattern and data acquisition pattern used in the verification test will be stated in section 4.

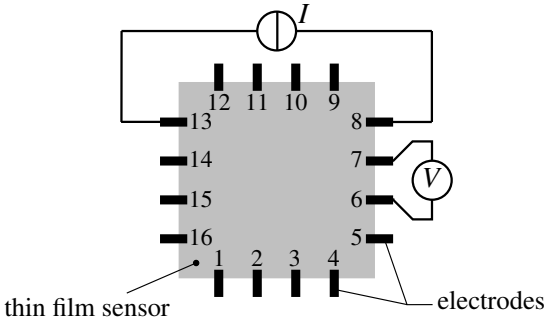

Figure 1: Sensor configuration and measurement pattern.

3. Data Acquisition Device

An Arduino™ Mega 2560 microcontroller is used to command the switch, measure the voltage, and read the measurement into a computer. It is a low-cost, open-source hardware that can be programmed with MATLAB/Simulink®. The Mega 2560 board has 54 digital input and output pins as well as 16 analog input pins. The board connects to a computer via a USB connection and is powered by an AC-to-DC adapter, which ensures an operating voltage of 5V. This causes the analog input signal to be limited within 0 to 5 V, and the digital signal is defined as High at 5 V and Low at 0 V.

3.1. Boundary Voltage Measurement

The boundary voltage is measured via two analog input pins (namely AI_1 and AI_2) from Arduino™ whereby the analog signal is converted into a 10-bit digital signal with a resolution of approximately 5 mV. To protect the analog-to-digital converter a voltage follower is implemented between the sensor and the analog inputs, as seen in Fig. 2. Due to the aforementioned limitation on voltage range taken by the AI pins, the boundary voltage signals are not measured directly between two neighboring electrodes.

Excerpt from ISBN 978-3-00-053387-7

Instead the voltage between each electrode and a ground point is measured, ensuring that the measuring signal is between 0 to 5 V. The voltage signal between two neighboring electrodes $U_{i,i+1}$ is therefore calculated as

$$U_{i,i+1} = U_i - U_{i+1}. \tag{6}$$

These voltage measurements are read and saved into a file using MATLAB® for EIT analysis.

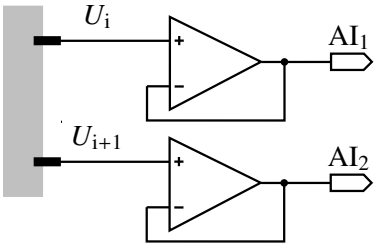

Figure 2: Arrangement of the boundary voltage measurement of two neighboring electrodes.

3.2. Voltage-controlled Current Source

In addition to the boundary voltage measurement, it is also necessary to have a reliable current source. The current source shall provide a continuously steady and precise electrical excitation to the sensor under various loading situation to ensure an unbiased voltage response. In this study a Howland current source scheme is chosen due to its ability to provide constant current flow to a given load. A voltage-controlled current source (VCCS) with grounded load was realized, as seen in Fig. 3. A reliable Howland current source requires all resistors to have the exact measurement of resistance; therefore the resistor's precision can significantly influence the stability and accuracy of the VCCS output. Resistors with higher precision are usually more expensive, therefore the compromise between cost and quality determines the choice of resistors. In this study resistors with an accuracy of 1% are chosen to generate a direct current between 0 to 5 mA with a resolution of 0.01 mA, and a potentiometer R_0 is used to regulate the current magnitude.

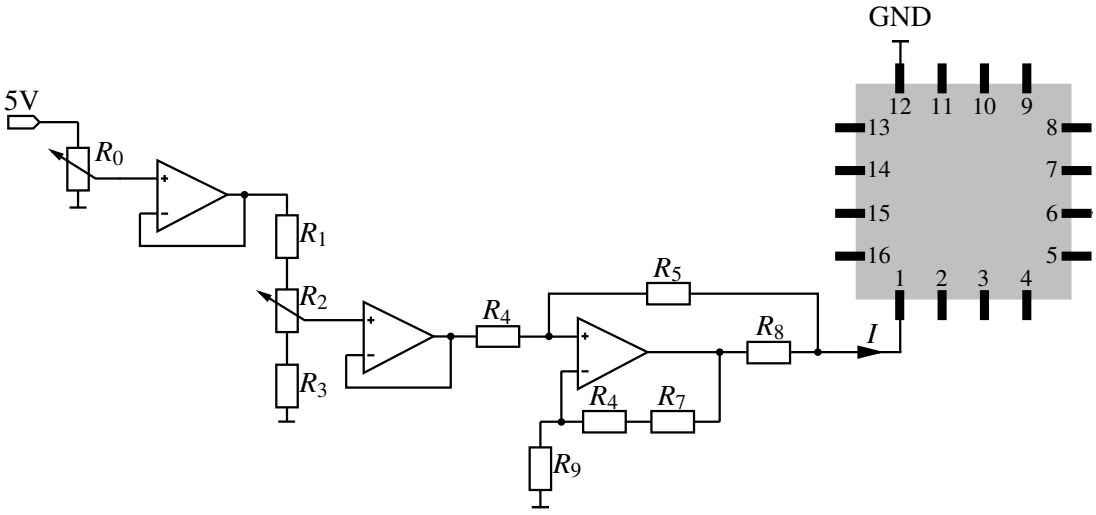

Figure 3: The circuit scheme of the Howland current source designed in this study.

Excerpt from ISBN 978-3-00-053387-7

3.3. Switch

A multi-port switch consisting of four high-speed CMOS logic analog 16:1 multiplexers CD74HC4067 from Texas Instruments, as depicted in Fig. 4, is chosen for this study. Two of the multiplexers are for switching among different pairs of electrodes with the current source connection (MUX1 and MUX2) and the other two are for voltage measurement (MUX3 and MUX4). Each multiplexer is controlled by four digital-control pins (DO's) via a binary-coded decimal (BCD) encoding; therefore it is possible to switch among 16 units to the designed output port (OUT). This allows any arbitrary patterns of current injection/voltage measurement to take place over a 16-electrode configuration. The available digital output pins from the Mega 2560 board are used to control the multiplexers, whereby the switching configuration of current injection and voltage measurement are programmed with the Arduino™ board. It should be noted that each multiplexer has an "on" resistance of about $R_{\text{on}} \approx 70\,\Omega$ connecting in series with the sensor's impedance. The resistance may vary while the circuit is connected, but it is negligible comparing to the signal's magnitude, as demonstrated by the reconstitution results shown in the following section.

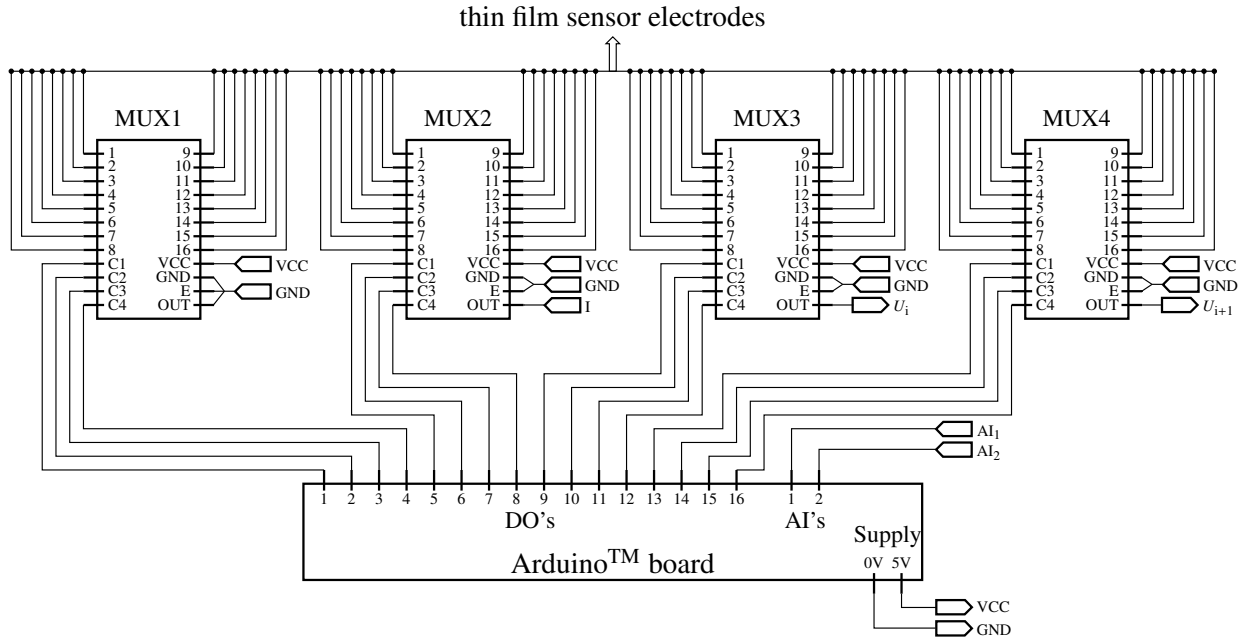

Figure 4: Configuration of the CMOS switch and Arduino™ Mega 2560.

3.4. Graphical User Interface

In order to visualize the EIT reconstruction result in a quasi real-time manner, access and control the input parameters in a more user-friendly environment, a MATLAB®-based graphical user interface (GUI) for performing EIT measurement/analysis is developed. Fig. 5 shows the typical appearance of the GUI, which consists of five major areas as numbered. The first area (1) initiates the precalculation process. Pressing down the "Precalculation" button will start EIDORS to construct an FEM model for the defined sensing area, generating the forward calculation result with an assumed constant conductivity shown in the plot to the right. In the next step the input current magnitude shall be defined, as seen in area (2). A turning knob is available on the current source circuit board to edit the input current magnitude in a range of 0 to 5 mA, which as a result will display in the box. A baseline measurement, or a measurement of the boundary voltage responses of the "healthy" structure can be taken at this moment or earlier. At

Excerpt from ISBN 978-3-00-053387-7

this moment all the tasks prior to an EIT evaluation are done, and a quasi real-time EIT reconstruction can take place at any desired moment. By clicking on the ”Run” button in area (4), a boundary voltage measurement will be taken again and displayed in the plot in area (3), followed by an immediate reconstruction calculation. The calculated EIT result will be displayed in area (5). The data acquisition process takes 2.56 s with a defined switch interval of 0.01 s for a 16-electrode configuration, and the calculation takes 5 to 6 s. The entire EIT evaluation takes 7 to 8 s, which allows a quasi real-time observation of the structure with respect to the long time monitoring task. The EIT evaluation can be repeated as often as necessary.

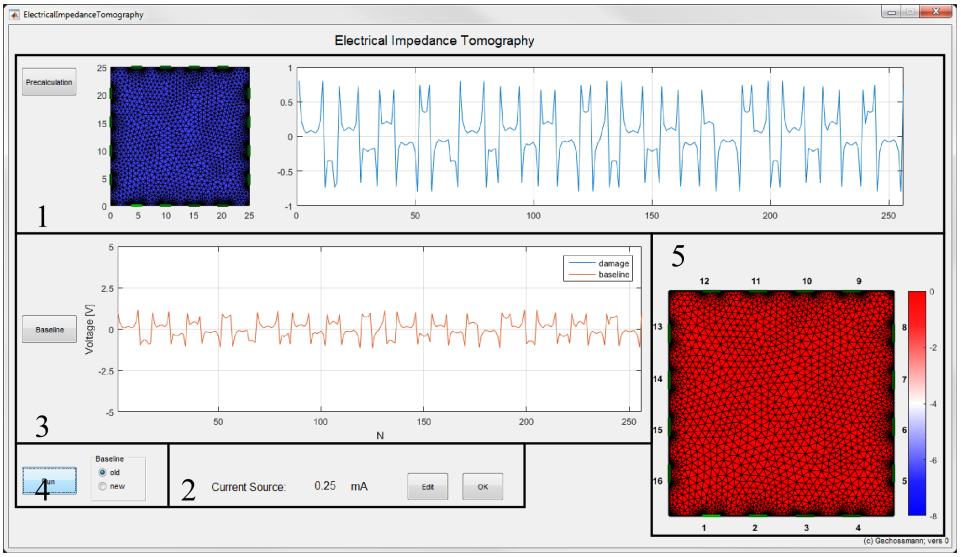

Figure 5: EIT graphical user interface.

4. Demonstration

To demonstrate an EIT evaluation with the developed data acquisition device, a bending test of a self-developed, inkjet-printed piezoresistive thin film sensor was performed (see Fig. 6) [7]. Because of the piezoresistivity, it is expected that the induced bending strains change accordingly to the conductivity, which should consequently be visualized in the EIT evaluation. The sensor has a dimension of 40 × 40 mm^2 and was printed on a commercial glossy photo paper. The 16 electrodes were connected to two 8-pin FFC sockets which were wired to the switch ports. The measurement procedure was taken with a current of $I = 0.25$ mA, and it was first applied between two electrodes that are facing against each other, *i.e.*, electrode 1 and 12. Starting from electrode 1, voltage measurements between neighboring electrodes (*i.e.*, 1 and 2) were taken within 0.01 s for 10 times. The voltage measurement was then switched to the next pair (2-3) to perform the same measurement until all 16 measurements were taken. The current injection was then switched to the next pair of electrodes (2-11), taking voltage measurements in the similar manner. By the end of the data acquisition process a total of 2560 measurements were taken within 2.56 s, and a reconstruction calculated was followed. In this study a total of four reconstructions were processed, each with a different bending situation as seen in Fig. 6. The reconstruction results are presented in Fig. 7.

Fig. 7 shows that the bending of the paper results in a negative contrast which is in good agreement with the fact that a tensile strain distribution is taking over the thin film. Furthermore, the negative contrast clusters in the middle span of the image, which is in correspondence to the maximum tensile strain region shown in Fig. 6. As the bending increases, which results in a larger maximum tensile strain

Excerpt from ISBN 978-3-00-053387-7

in the center, the contrast also gets higher in magnitude and spreads to a larger extend, as observed in Fig. 7(b) to Fig. 7(d). One can also observe that there is a big difference of contrast between top/bottom of the bending area and the center; this might correlate to the effect of upward bending of the paper's top/bottom edges due to the free boundary condition. However, it should be noted that the sensor is not calibrated at this moment, as the contrast change value is not correlated to the strain magnitude yet. It also seems that the contrast change due to strain is not linear.

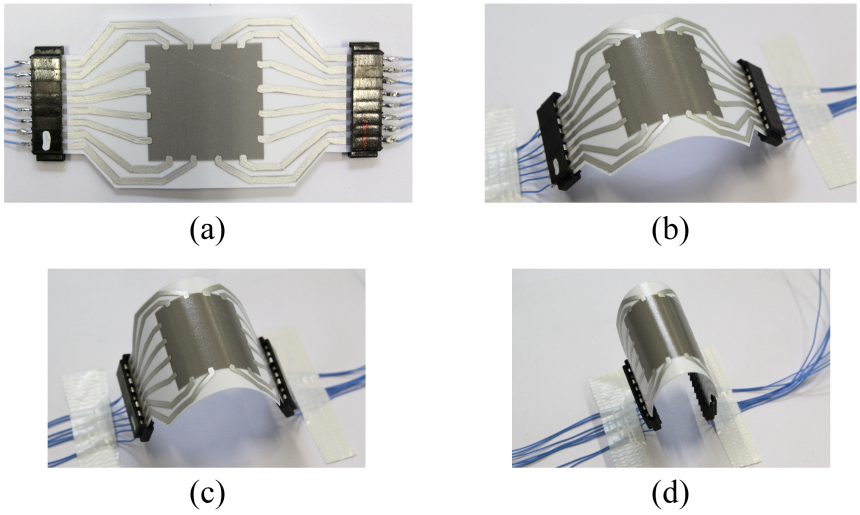

Figure 6: Bending status of the paper-sensor (a) no bending, (b) bending state 1, (c) bending state 2 and (d) bending state 3.

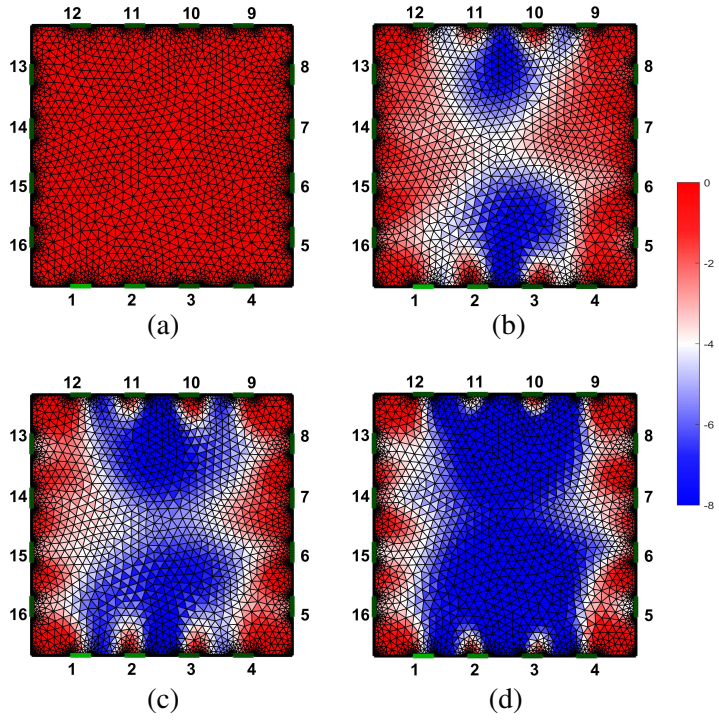

Figure 7: Reconsturction (a) no bending, (b) bending state 1, (c) bending state 2, and (d) bending state 3.

Excerpt from ISBN 978-3-00-053387-7

5. Conclusion

In this study a self-developed hardware for spatial damage identification and strain distribution reconstruction electrical impedance tomography is developed. Coupled with an inkjet-printed carbon nanotube thin film, the device is able to control current injection, read and save voltage measurement to a computer with desired precision. Together with a MATLAB®-based graphical user interface, the device can support a quasi real-time EIT evaluation over a 16-electrode spatial sensor under 9 s. The speed can be further improved by taking voltage measurement simultaneously per current injection. Other planned improvement of the device include increasing the number of switching channels, as well as improvement upon the range and precision of voltage measurement, so that it can support EIT evaluations over a larger structure.

Acknowledgments

The financial support by the Austrian Federal Ministry of Economy, Family and Youth and the National Foundation for Research, Technology and Development is gratefully acknowledged. The authors are grateful to Erich Humer for his technical support during the experiments.

References

[1] National Transportation Safety Board Bureau of Accident Investigation Washington. Aircraft Accident Report–Aloha Airlines, Flight 243, Boeing 737-200, N73711, near Maui, Hawaii, April 28, 1988. Technical Report NTSB/AAR-89/03, 1989.

[2] V. Esslinger, R. Kieselbach, R. Koller, and B. Weisse. The railway accident of eschede – technical background. *Engineering Failure Analysis*, 11:515–535, 2004.

[3] V. Giurgiutiu. *Structural Health Monitoring with Piezoelectric Wafer Active Sensors*. Academic Press, 2nd edition, 2014.

[4] K. J. Loh, T. C. Hou, J. P. Lynch, and N. A. Kotov. Carbon Nanotube Sensing Skins for Spatial Strain and Impact Damage Identification. *Journal of Nondestructive Evaluation*, 28(1):9–25, 2009.

[5] B. H. Brown, D. C. Barber, and A. D. Seagar. Applied potential tomography: possible clinical applications. *Clinical Physics and Physiological Measurement*, 6:109–121, 1984.

[6] A. Adler and R. Guardo. Electrical impedance tomography: regularized imaging and contrast detection. *IEEE Transactions on Medical Imaging*, 15(2):170–179, 1996.

[7] Y. Zhao, C. Beisteiner, S. Gschossmann, and M. Schagerl. A inkjet-printed carbon nanotube spatial strain sensor for quasi real-time health monitoring of lightweight design materials. In *7th Forum on New Materials (part of CIMTEC 2016)*, Advances in Science and Technology. Trans Tech Publications Inc., 2016.

Excerpt from ISBN 978-3-00-053387-7